

Interactions between an ABS type leadless glaze and a biscuit fired bone china body during glost firing. Part II: investigation of interactions

Alpagut Kara^{a,*}, Ron Stevens^b

^aAnadolu University, Department of Ceramic Engineering, Eskişehir, Turkey

^bDepartment of Engineering and Applied Science, University of Bath, Bath, UK

Received 16 February 2001; received in revised form 10 July 2001; accepted 16 July 2001

Abstract

This part of the study involves the investigation of the interactions between an ABS type commercial leadless glaze and a biscuit fired bone china body during glost firing at different temperatures using XRD and SEM techniques. The aim was to obtain detailed and systematic information about the morphological and chemical characteristics of the resultant phases formed at the interfaces. Separate examination of the interactions between the glaze and the experimental crystalline phases of the body prepared earlier, namely anorthite and β -TCP, were also carried out in an effort to show their susceptibility to react with the glaze independently. As a result, the presence of a range of interaction layers with distinctly different morphological and chemical characteristics was successfully demonstrated. It was proposed that β -TCP was the major contributor to the overall interactions by reacting with CaO from the glaze in the presence of water vapour and forming hydroxyapatite crystals at the glaze-body interfaces. Although the exact origin for the development of water vapour in the molten glaze could not be determined, several potential sources were suggested.

© 2002 Elsevier Science Ltd. All rights reserved.

Keywords: Anorthite; Apatite; Bone china; $\text{Ca}_3(\text{PO}_4)_2$; Glaze; Interfaces

1. Introduction

Lead, in one form or another, has been used for a very long time. However, it was not until the 1750's that lead release from pottery was recognised as a problem. Josiah Wedgwood knowing that raw lead glazes were improper for preserving acid fruits and pickles declared "I shall try to make a glaze without lead", but he failed.¹ Introduction of strict lead release limits on tableware started mainly in Finland in the late 1960's. Since then lead release limits have been constantly reviewed both in the UK and the USA and lower and lower levels have been introduced. Consumer and environmental concerns about the use of lead in tableware glazes and decoration have been raised, particularly in the USA, by the combination of two factors.² Firstly, a growing body of medical studies on the toxic

city of lead which indicates that even very low levels of lead in the bloodstream can be harmful to children, and secondly, a well publicised case of severe lead poisoning of the Wallace family from America in the late 1980s attributed to craft-type pottery originating from Italy. As a result of stringent lead release limits, the tableware industry has started to move towards the use of leadless glaze and decoration systems. The main leadless glaze systems, which have emerged as practical technologies are advanced borosilicate glazes (ABS), low and high bismuth glazes and zinc–strontium glazes.^{2–4}

The most common approach in the development of leadless glazes has been to completely remove lead oxide from the composition and make up the difference with the remaining and additional oxides such as MgO, ZnO and ZrO₂. These types of glaze have become known as ABS glazes. ABS glazes have a lower refractive index in comparison to bismuth and lead based systems, and thus appear less glossy. Moreover, they are significantly more viscous and have poorer body wetting characteristics. The flow properties and healing characteristics of

* Corresponding author. Tel.: +90-222-321-3550; fax: +90-222-32 39501.

E-mail address: akara@anadolu.edu.tr (A. Kara).

these glazes can be improved using a higher glost firing temperature. However, there is a limit to the benefits that can be achieved by raising the temperature. ABS glazes should not be fired above ~ 1150 °C because volatilisation of boron and alkali oxides can become significant. The method of application is also critical in order to achieve better glaze appearance and acceptable glost firing yields. If high glost yields cannot be achieved, then the cost benefit of ABS glazes over bismuth based glazes is lost, and bismuth glazes may well prove more cost-effective overall.

To date, ABS glazes have been developed for earthenware, hotelware, and bone china bodies. These glazes are particularly promising on high thermal expansion bodies such as bone china, giving good gloss and durability. Application to low thermal expansion bodies such as earthenware is, however, more difficult because low thermal expansion glazes of this type generally exhibit higher viscosity resulting in poor flow during glost firing and consequently poor appearance. In economic terms, the ABS glazes are reported to be priced at virtually the same levels as their former lead equivalents. Therefore, most companies, when making a change to leadless glazes, start by looking at ABS glazes first and only proceed to more expensive bismuth glazes should their requirements not be met with the less expensive systems.

The present study was intended to obtain detailed and systematic information about the interactions and the morphological and chemical characteristics of the resultant phases formed at the interfaces between an ABS type leadless glaze and the biscuit fired bone china body previously studied by Kara and Stevens.^{5,6} The glost firing was undertaken at different temperatures with the aim of advancing understanding of the fundamental mechanisms of the reactions. The separate investigation of the interactions between the glaze and the experimental crystalline phases of the body was also attempted in order to show their susceptibility to react with the glaze independently.

2. Experimental

2.1. Material Preparation

A commercial ABS glaze was provided, in the powder form, by Ferro Ltd. (UK). The chemical composition of the glaze could not be supplied for reasons of commercial secrecy. Hence, the quantitative chemical analysis of the glaze was carried out by Ceram Research Ltd. (UK) using X-ray fluorescence spectroscopy (XRF) (See Table 1). Unfortunately, detection of boron in the composition was not possible. The remainder of the composition was assumed by difference to be boric oxide.

The specific gravity of the dry glaze was measured with a helium gas pycnometer (Micromeritics, Accupyc

Table 1
XRF analysis of the ABS glaze

Oxide	wt. %
SiO ₂	54.0
TiO ₂	0.07
Al ₂ O ₃	16.6
Fe ₂ O ₃	0.19
CaO	6.27
MgO	0.52
K ₂ O	3.29
Na ₂ O	5.13
P ₂ O ₅	0.07
Mn ₃ O ₄	0.02
ZrO ₂	1.21
HfO ₂	0.02
ZnO	0.01
BaO	0.08
SrO	0.08
B ₂ O ₃	10.1
LOI at 1025 °C	2.30

1330, USA) and found to be 2.5, which is an average value for typical leadless glazes. The glaze slip was set to a slop density of 1.55 kg/l. The viscosity measurements on the slip were carried out using a Torsion viscometer (Gallenkamp, England). The viscosity was adjusted to a value of approximately 195 overwing by the addition of Epsom salts (MgSO₄·7H₂O) in small amounts so that the desired fired thickness (~ 120 μm) could be obtained. Glaze application on the representative samples of the biscuit fired bone china body and the experimental crystalline phases was achieved by hand dipping.

The glost firings were carried out in an electric chamber furnace (Model: CWF 13/13, Carbolite, England). The glazed samples were fired at 1060 and 1120 °C with a soaking time of 1 h in order to follow the change of the interactions as a function of temperature. The heating and the cooling rates were 1.7 and 3.3 °C/min, respectively.

2.2. Techniques

For the XRD work, thin layers of the glaze were removed successively, parallel to the underlying substrate. This allowed the qualitative determination of the crystalline reaction products formed at the interfaces during glost firing. For this purpose, the representative specimens were bonded to the platform of a precision polishing jig with quartz wax and ground on an expanded polyurethane surface with 0.06 μm colloidal silica using a Logitech precision lapping and polishing machine (Model: PM4, Scotland, UK). Close control of the thickness of the glaze stock removal was achieved since the jig has a micrometer dial indicator attached. Frequent checks were also carried out using an optical microscope. A Philips PW 1710 based diffractometer

was employed with a 40 kV generator voltage and a 25 mA current. The scans were made over a range of 2θ values of $5\text{--}80^\circ$ with data acquisition occurring for 1.0 s, at intervals of 0.02° .

Microstructural and chemical examination of the polished and etched interfaces in cross-section and plan-view were carried out using a Jeol JSM-6310 analytical scanning electron microscope (SEM) equipped with Oxford Instruments AN 10/85 Link microanalysis system. Both secondary (SE) and back-scattered (BE) imaging modes were employed.

3. Results and Discussion

3.1. ABS glaze-biscuit fired bone china body interface

SEM examination of the representative polished cross-sections at lower magnifications did not reveal clear evidence of any interaction layer formation at both glaze firing temperatures. However, crystalline products at the interfaces can be distinguished at higher magnifications. Fig. 1 shows a typical BE image of such an interface glaze fired at 1120°C . The significant point to be observed on this image is the presence of needle-like crystals (marked with arrows). Another important feature is that the glaze layer is in contact mostly with what appears to be the β -TCP crystals, identified by their bright contrast. Fig. 2 is an EDS spectrum taken from the ABS glaze layer in Fig. 1. All elements present in the glaze composition were readily detected with the exception of B, confirming semi-quantitatively the XRF analysis results (see Table 1).

Fig. 3 is a SE image of an area similar to that in Fig. 1, after etching with 5% HF solution for 60 s. One of the main features of this micrograph is the presence of extensive numbers of small crystals, mostly in the form of aggregates of grains less than $1\ \mu\text{m}$ in diameter, embedded in the glaze layer at the interface. The EDS analyses on these crystals show the presence of mainly Ca and P with varying but lesser amounts of Si, Al and Na elements (see Fig. 4). The preferential accumulation of Ca and P at the interface is assumed to occur as a result of the reaction between P_2O_5 , either as-combined, as in the β -TCP phase, or as free phosphorus in the glassy matrix of the body, together with CaO from the glaze. This deduction may be made since P_2O_5 is the only oxide present in the body which is not present in the glaze. This assumption is in agreement with the results of Roberts and Beech,⁷ who evidenced the formation of an apatite phase at the interfaces between CaO containing glazes and a bone china body using XRD. The explanation given for this was also the favoured reaction between the β -TCP component of the body and the CaO from the glaze. In addition, they carried out their experiments with CaO free glazes and

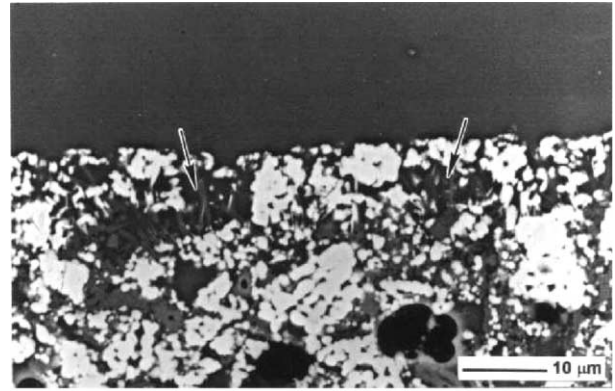


Fig. 1. A typical BE image of the polished cross-section of the ABS glaze-biscuit fired bone china body.

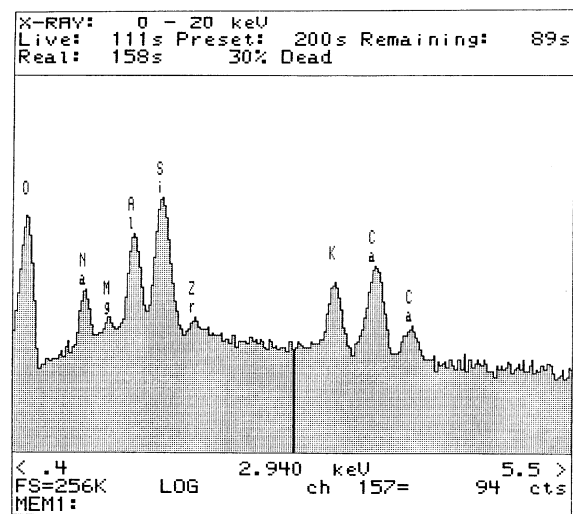


Fig. 2. A typical EDS spectrum of the ABS glaze layer.

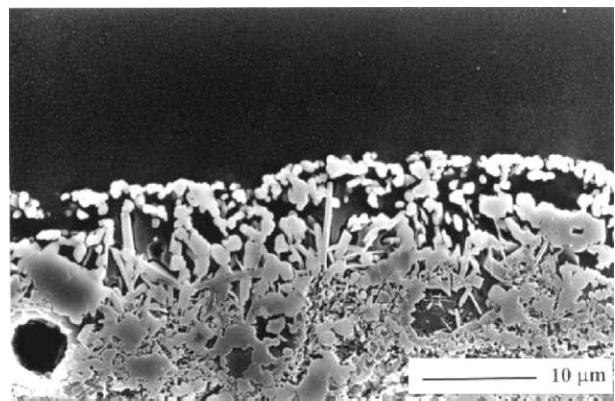


Fig. 3. A typical SE image of the polished and etched cross-section of the ABS glaze-biscuit fired bone china body.

found that no apatite phase formed at the interface. In a later study by Ichiko,⁸ hydroxyapatite was observed at the interfaces between different types of glazes and a bone china body.

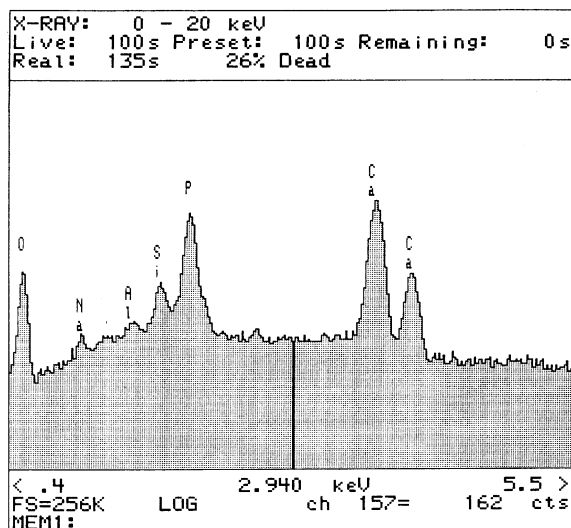


Fig. 4. A typical EDS spectrum of the granular grains embedded in the glaze at the ABS glaze-biscuit fired bone china interface.

Regarding the needle-like crystals at the interface in Fig. 3, EDS analyses reveal that they contain Al, Si and Ca with lesser amounts of Na and K. Fig. 5 illustrates such a spectrum. The F peak in the spectrum is assumed to be a result of remnant contamination after etching with HF solution.

Similar morphological and chemical characteristics were observed for the ABS glaze-biscuit fired bone china body interfaces glost fired at 1060 °C, but to a lesser degree.

A representative XRD spectrum of the ABS glaze-biscuit fired bone china body interface glost fired at 1120 °C is illustrated in Fig. 6. In order to emphasise the presence of the peaks related to the crystalline phases formed at the interface, the spectrum is also compared with that of the body itself. As can be seen, most of the peaks on the interface spectrum originate from the underlying body, thus making interpretation difficult. A significant amount of amorphous background scattering is also evident due to the presence of remnant glaze. Close examination of the XRD spectrum of the interface revealed that several new peaks emerged which do not belong to the crystalline components of the body. Comparison with the standard references indicates that the peaks can be attributed to hydroxyapatite ($\text{Ca}(\text{OH})_2 \cdot 3\text{Ca}_3(\text{PO}_4)_2$), (JCPDS-ICDD No: 09-432). Moreover, some of the hydroxyapatite peaks are observed to overlap with those from the β -TCP phase of the body. The interface spectrum did not show any distinctive peak or peaks related to the needle-like crystals. The presence of these at the interfaces was appeared to be limited in comparison to the quantity of granular crystals by SEM. Thus, detection by XRD in such a small amount would be expected to be difficult. It is also likely that the representative peaks may overlap with the

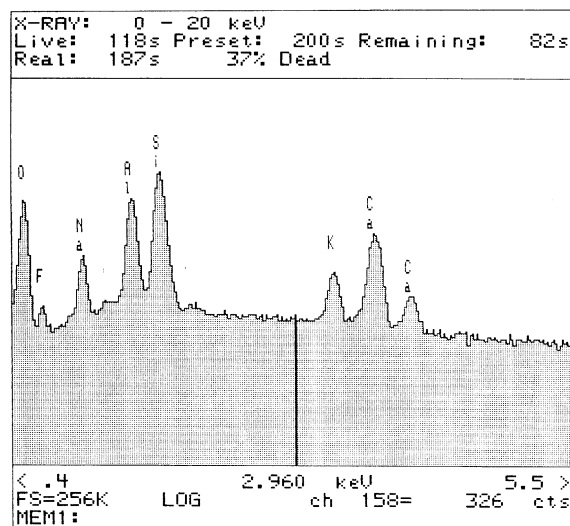
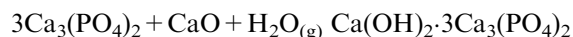


Fig. 5. A typical EDS spectrum of the needle-like crystals at the ABS glaze-biscuit fired bone china interface.

peaks from the anorthite phase present in the body, due to their similar chemistry.

The nucleation and growth of the hydroxyapatite crystals at the interfaces during glost firing can proceed according to the following reaction:



Evidence for this reaction also comes from a study by Monma and his co-workers.⁹ They reported hydroxyapatite formation between 850 and 1200 °C during heating of a stoichiometric mixture of $\text{Ca}_2\text{P}_2\text{O}_7$ and CaCO_3 in air and suggested that the reaction of the mixture with atmospheric water vapour was responsible. In another study, Monma and Kanazawa¹⁰ studied the thermal formation of hydroxyapatite from $\text{Ca}_3(\text{PO}_4)_2$ and CaO in the presence of water vapour and showed that the conversion of $\text{Ca}_3(\text{PO}_4)_2$ to hydroxyapatite reached 100% within 50 min at 1300 °C.

Although the exact source of H_2O in the reaction above is not known, several possibilities can be suggested. One possibility is the water released as a result of the decomposition of certain glaze components during glost firing. Water vapour can also be entrapped by rapid melting and sealing of the glaze. However, this is a particular problem when excessively fast glost firing cycles are used. Frits are another source of water. Although frits are considered to be insoluble in water, all glasses react to an aqueous environment and they possess a small but measurable solubility. The solubility of water in frits was reported to be of the order of 0.1–0.3%, detected using infrared spectroscopy.¹¹ Taking these possibilities into account, the development of a water vapour pressure in the molten glaze and its participation in the formation of the hydroxyapatite crystals at the interfaces during glost firing can then be explained.

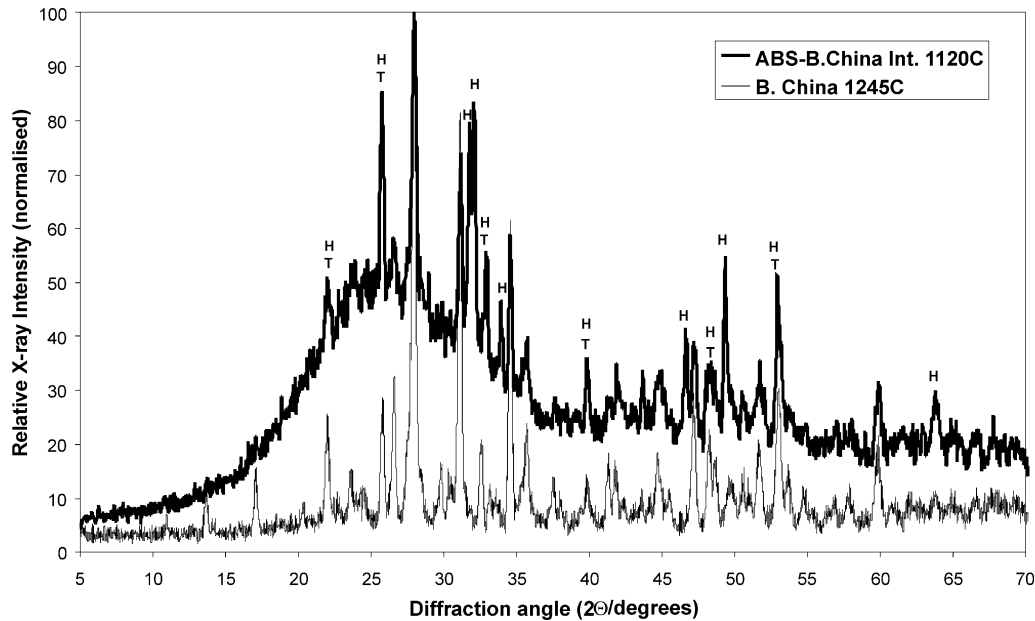


Fig. 6. A comparison of the XRD spectrum of the ABS glaze–biscuit fired bone china interface with that of the biscuit fired bone china (T: β -TCP, H: hydroxyapatite).

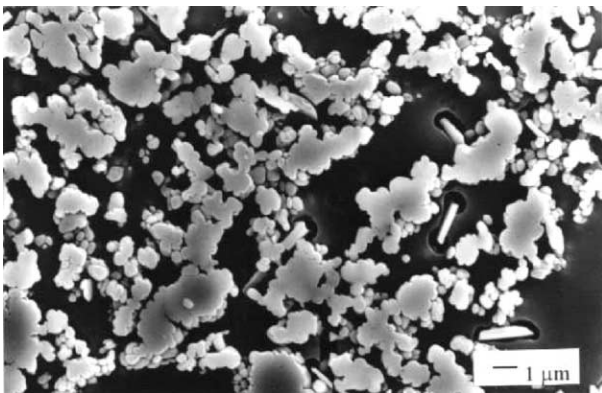


Fig. 7. A typical SE image of the ABS glaze–biscuit fired bone china body interface (polished and etched top surface).

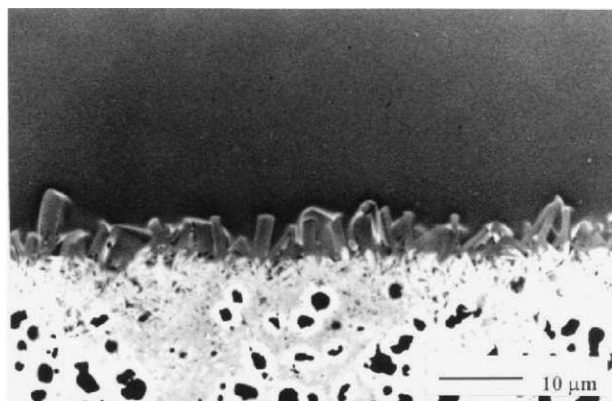
Fig. 7 shows a plan-view SE image of the ABS glaze–biscuit fired bone china body interface following etching with 5% HF solution for 60 s. This image was taken from the same surface used to generate the XRD spectrum in Fig. 6. As a result of the etching, the existence of granular crystals at the interface, is clearly revealed. There are also several needle-like crystals present in the image. As compared to the cross-sectional image previously depicted in Fig. 3, this technique provides a far more detailed picture of the interaction layer, particularly in terms of the distribution and morphology of what proposed to be hydroxyapatite crystals.

3.2. ABS Glaze-experimental anorthite interface

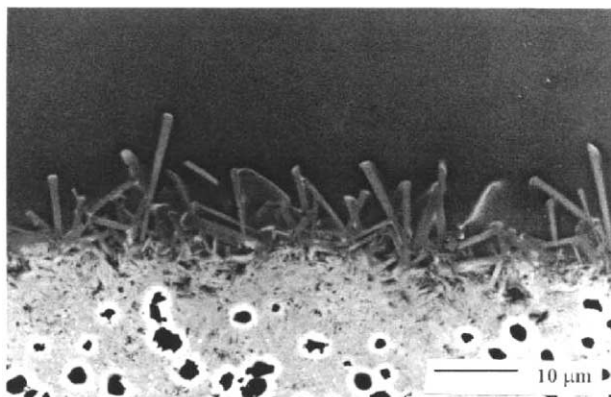
SEM observations on the representative polished cross-sections revealed a well-developed interaction

layer at both glaze firing temperatures. Fig. 8(a) and (b) exhibit typical BE images of such interfaces. These images provide sufficient atomic number contrast to infer that the interaction layer consists of needle-like crystals with different lengths and thickness growing into the glaze at different directions from the anorthite. It is also clear from the images that the thickness of the interaction layer increases with the glaze firing temperature.

Etching the polished cross-sections of the relevant specimens with 5% HF solution for 60 s showed that the etchant selectively attacked the anorthite substrate and the glassy phase around the needle-like crystals at the interface. It left the crystals and the glaze untouched, consequently revealing the morphology of the interaction layer. Fig. 9 illustrates a typical SE image of such an etched interface. The EDS analyses on the individual needle-like crystals show the presence of Al, Si, Ca, and Na with a small amount of K (see Fig. 10). When compared to the substrate, the interface crystals contain more Si and less Al and Ca with considerable amount of Na. It is proposed that these crystals are formed as a result of the ionic diffusion of Na and Si into the anorthite and substituting Ca and Al in its lattice during glaze firing. The presence of a small amount of K may be due to its diffusion from the glaze or signal interference from surrounding areas. It is important to mention here that the EDS spectrum given in Fig. 10 is very similar to the spectrum in Fig. 5, which was taken from a needle-like crystal at the ABS glaze–biscuit fired bone china body interface. This suggests that these crystals, in addition to having the same morphology, appear to have similar chemical composition. Anorthite



(a) glost fired at 1060 °C



(b) glost fired at 1120 °C

Fig. 8. Typical BE images of the polished cross-sections of the ABS glaze-experimental anorthite interface (a) glost fired at 1060 °C (b) glost fired at 1120 °C.

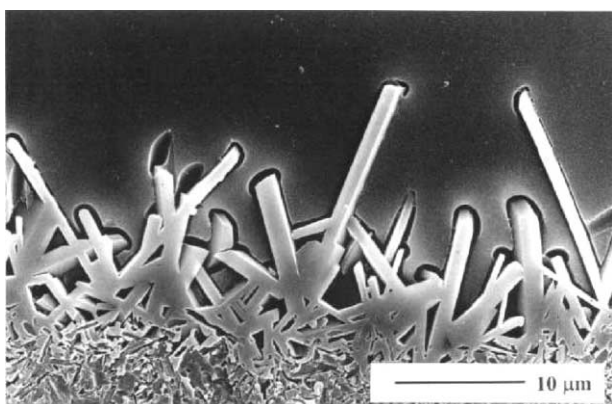


Fig. 9. A typical SEI image of the polished and etched cross-section of the ABS glaze-experimental anorthite interface (glost fired at 1120 °C).

is the lime-rich end member of the plagioclase feldspars. This type of feldspars consists of a continuous series of solid solutions between anorthite ($\text{CaO} \cdot \text{Al}_2\text{O}_3 \cdot 2\text{SiO}_2$) and albite ($\text{Na}_2\text{O} \cdot \text{Al}_2\text{O}_3 \cdot 6\text{SiO}_2$), in all proportions, at all temperatures.¹² Consequently, the interface crystals are expected to have an intermediate composition between

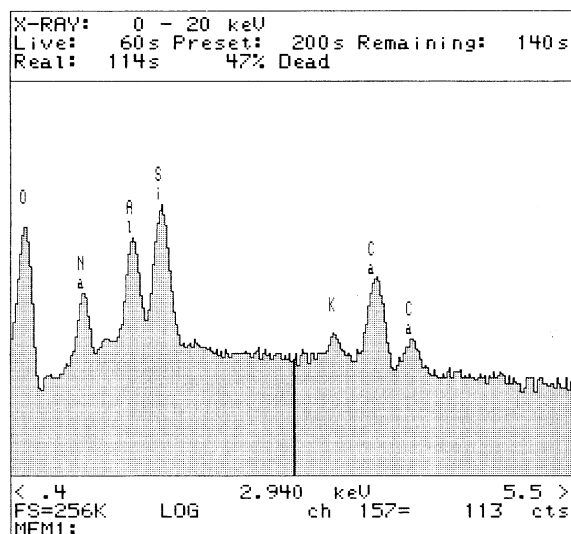


Fig. 10. A typical EDS spectrum of needle-like crystal at the ABS glaze-experimental anorthite interface (glost fired at 1120 °C).

anorthite and albite. The formation of such interface crystals with similar chemistry and morphology, between a lead containing glaze and an anorthite body, was reported previously by Ruddlesden.¹³

The thickness of the interaction layer was observed to enlarge with increasing glost firing temperature. Because the interaction layer was found to have a chemical composition different from that of the glaze and the anorthite, its nucleation and growth can be treated as the formation of a new phase. Such growth must involve the diffusion of the ions through the interface from the glaze into the anorthite and vice versa.

Fig. 11 gives a comparison of the XRD spectrum of the ABS glaze-experimental anorthite interface glost fired at 1120 °C with that of the experimental anorthite. As can be seen, the interface spectrum consists mainly of the underlying anorthite. No new peaks emerged due to the presence of the needle-like crystals at the interface.

Fig. 12 illustrates a plan-view SE image of the same interface etched with 5% HF solution for 30 s where the XRD spectrum in Fig. 11 was taken from. A network of the needle-like crystals embedded in the glaze can be clearly seen, demonstrating the relevance of the spectrum.

3.3. ABS glaze-experimental β -TCP interface

SEM study of the representative polished cross-sections revealed the development of an interaction layer at both glost firing temperatures. Fig. 13(a) and (b) are typical BE images of such interfaces. The continuous bright layer marked with arrows is believed to be the interaction layer. However, it is difficult to make

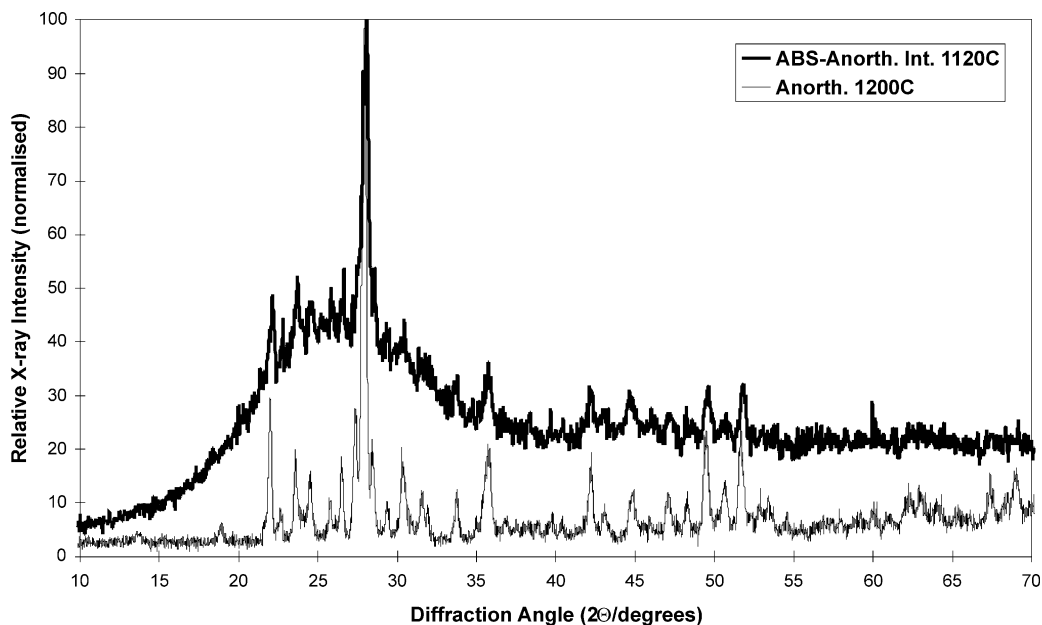


Fig. 11. A comparison of the XRD spectrum of the ABS glaze-experimental anorthite interface with that of the experimental anorthite.

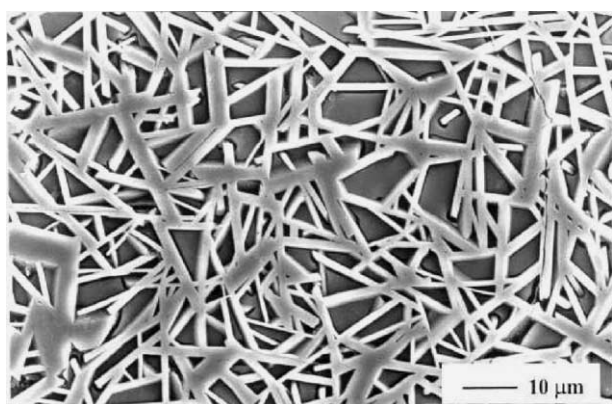


Fig. 12. A typical SE-image of the ABS glaze-experimental anorthite interface (polished and etched top surface).

significant comments about the morphology of the interaction layer from such images. A slight increase in the thickness of the interaction layer with glost firing temperature is also apparent.

As a result of etching the polished cross-sections of the relevant specimens with 10% glacial acetic acid solution for 120 s revealed that the etchant preferentially attacked the interaction layer and the β -TCP substrate, but left the glaze layer untouched. Fig. 14 gives a typical SE image of such an etched area. As can be seen, the interaction layer has similar form as the bulk of the β -TCP substrate but it is less susceptible to the etching process. It appears to consist of individual crystalline grains grown into the underlying substrate. The EDS analyses on the interaction layer show the presence of mainly P and Ca. There are also small amounts of Na and Si present, which is evidence that ionic diffusion was taken place from the glaze into the

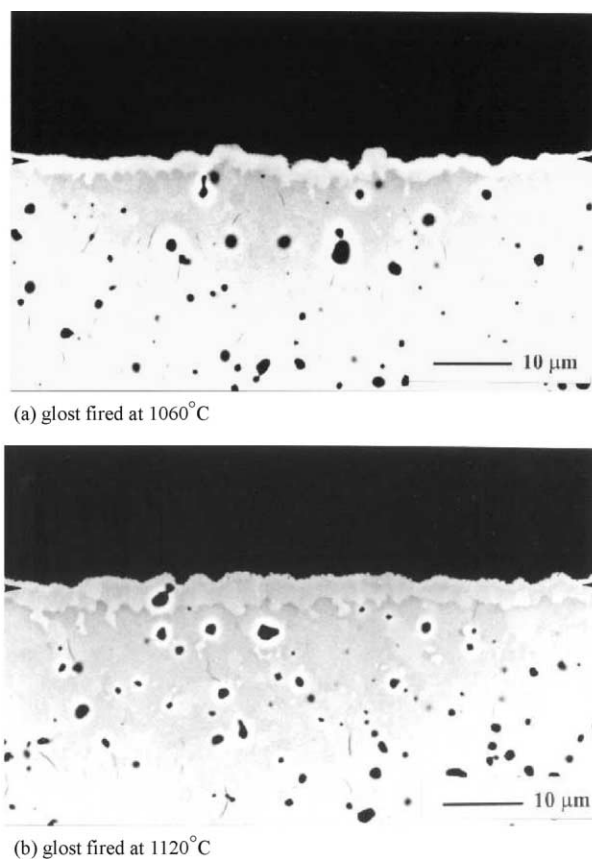


Fig. 13. Typical BE images of the polished cross-sections of the ABS glaze-experimental β -TCP interface (a) glost fired at 1060 °C (b) glost fired at 1120 °C.

substrate during glost firing, Fig. 15. It is worth pointing out the similarity of this spectrum to that taken from the granular grains at the ABS glaze-biscuit fired

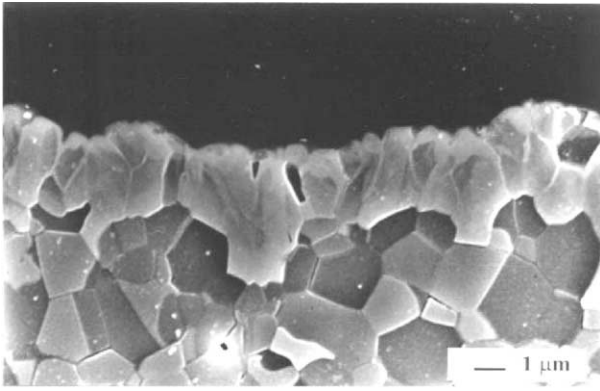


Fig. 14. A typical SEI image of the polished and etched cross-section of the ABS glaze-experimental β -TCP interface (glost fired at 1120 °C).

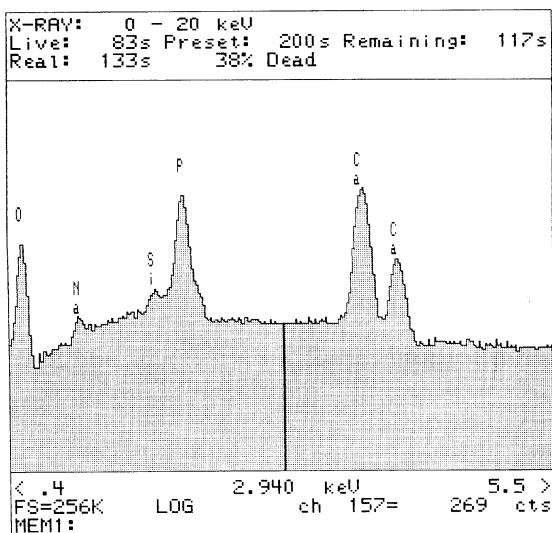


Fig. 15. A typical EDS spectrum of the interaction layer at the ABS glaze-experimental β -TCP interface.

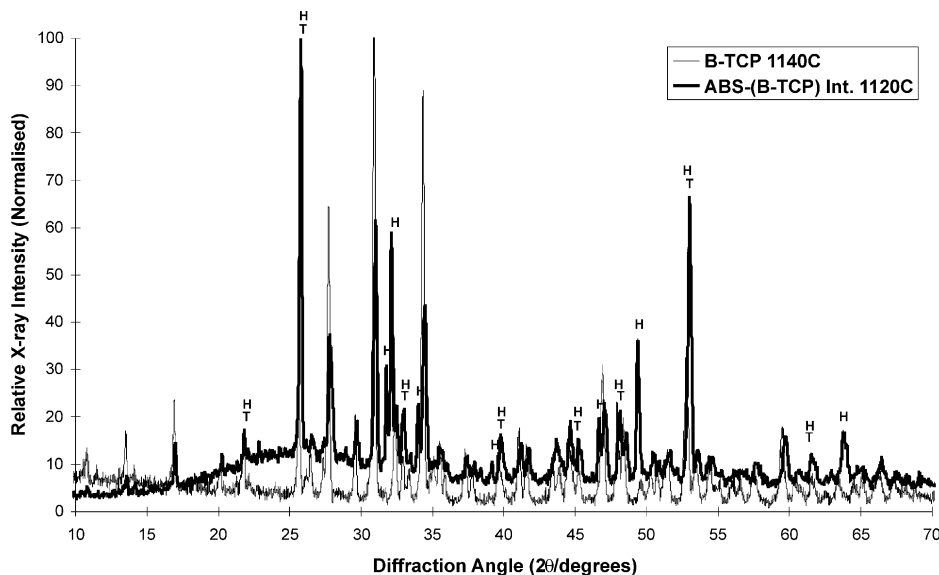


Fig. 16. A comparison of the XRD spectrum of the ABS glaze-experimental β -TCP interface with that of the experimental β -TCP (T: β -TCP, H: hydroxyapatite).

bone china interface, Fig. 4. These observations support the proposal that the reaction between the β -TCP component of the bone china body and the glaze results in the formation of a calcium phosphate rich phase at the interface during glost firing.

Fig. 16 is a representative XRD spectrum of the ABS glaze-experimental β -TCP interface glost fired at 1120 °C. In order to emphasise the presence of the peaks related to the crystalline phases at the interface, the spectrum can be compared with that of experimental β -TCP, where a reasonable coincidence occurs. A high background due to the presence of remnant glaze is also observable. Close examination of the interface spectrum revealed the presence of several new peaks, which do not belong to the underlying β -TCP. As a result of comparison with the standard reference patterns, it was concluded that these peaks are related to hydroxyapatite. Of further interest, some of the peaks ascribed to hydroxyapatite are located at the same position as those of the β -TCP. Hydroxyapatite was previously detected by XRD at the ABS glaze-biscuit fired bone china interfaces (see Fig. 6). Fig. 17 shows a comparison of the XRD spectrum of the ABS glaze-experimental β -TCP interface with that of the ABS glaze-biscuit fired bone china body interface and it is clear that the hydroxyapatite peaks from both spectra correlate closely. This again can be taken as further supportive evidence for the preferential reaction between the β -TCP phase of the body and CaO from the glaze layer.

Fig. 18, a plan-view SE image of the ABS glaze-experimental β -TCP interface after etching with 5% HF solution for 60 s, shows crystalline grains having different particle sizes, ranging from 0.5 to 2.5 μ m. There are also unetched areas of the interaction layer evident in the field of the micrograph. Moreover, several glaze

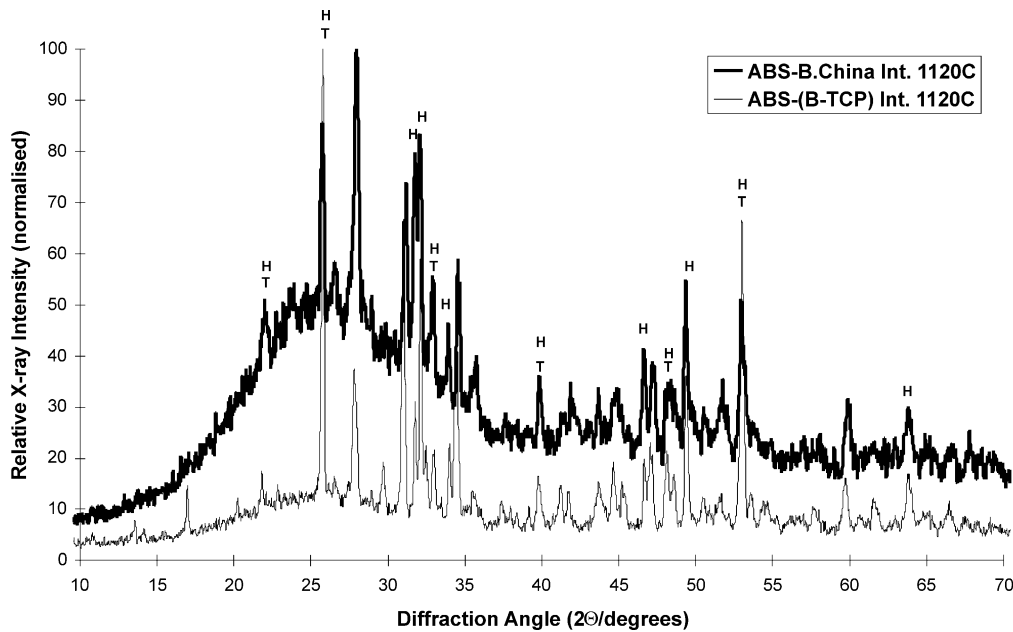


Fig. 17. A comparison of the XRD spectrum of the ABS glaze–experimental β -TCP interface with that of the ABS glaze–biscuit fired bone china interface (T: β -TCP, H: hydroxyapatite).

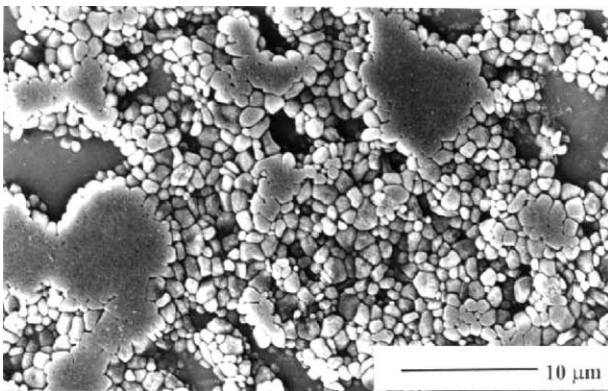


Fig. 18. A typical SEI image of the ABS glaze–experimental β -TCP interface (polished and etched top surface).

pockets are present due to the unevenness of the surface and different depth of glaze penetration. Formation of a continuous interaction layer, consisting of individual crystalline grains at the ABS glaze–experimental β -TCP interfaces had previously been illustrated on the relevant cross-sectional specimen (see Fig. 14). It is important to note that the chemical etchant used for this purpose was 10% glacial acid solution. Although this type of etchant was found to be efficient enough to exhibit the different structure of the interaction layer compared to the underlying substrate, the exact morphology of the individual grains forming the interaction layer was not quite revealed. In contrast, the technique of etching the polished top surface of the interface region with 5% HF solution provides a better etch and a clear appreciation of the nature of the interaction layer.

4. Conclusions

The combined use of XRD and mainly SEM techniques suffice to determine within reasonable limits that a range of interaction layers with distinctly different morphological and chemical characteristics occurs at the interfaces between the ABS type leadless glaze and the biscuit fired bone china body and its experimental crystalline phases as a function of glaze firing temperature. These interaction layers can be divided into three classes as follows.

The first type of interaction layer was observed between the ABS glaze and the biscuit fired bone china body, characterised by the glaze penetrating into the body and filling the closed pores, to make a non-porous layer, which then gives rise to the formation of calcium phosphate rich granular crystals at the interfaces. Indeed, hydroxyapatite was indicated by XRD. The formation of such crystals was suggested to take place as a result of the reaction between P_2O_5 , either as-combined, as in the β -TCP phase, or as free phosphorus in the glassy matrix of the body, together with CaO from the glaze. A further important observation was the presence of the needle-like crystals at the interfaces between the glaze and the body. These crystals show a close resemblance to those observed when the same glaze was glaze fired on the experimental anorthite, in terms of their morphology and chemical composition, indicating a separate reaction between the anorthite phase of the body and the glaze.

A second class of interaction layer was found between the ABS glaze and the experimentally prepared anorthite, characterised by the formation of a layer of needle-like crystals growing into the glaze from the

anorthite at the interfaces. It is believed that Na and Si ions diffuse into the underlying anorthite and substitute Ca and Al in its lattice structure with the consequent formation of these crystals. These same crystals were also found to be present at the interfaces when the same glaze was glost fired on the bone china body in this study. This is evidence that Na and Si present in the glaze diffuse into the bone china body and react independently with the anorthite phase at the interface, to form such crystals during glost firing. However, there was the lack of any additional peak or peaks on the relevant XRD spectrum due to the presence of these crystals.

The third class of interaction layer was established between the ABS glaze and the experimentally prepared β -TCP, characterised by the formation of a continuous layer of individual crystalline grains at the interfaces. Using XRD, the grains were identified as hydroxyapatite, supporting the proposal that the calcium phosphate rich crystals embedded in the glaze at the interface are formed as a result of the preferential reaction, in the presence of water vapour, of the β -TCP component of the biscuit fired bone china body and CaO from the glaze.

In regard to the contribution of the glassy matrix phase to the formation of the interaction layers, it is believed that the glassy phase plays a significant role by helping the formation of a low viscosity melt together with the glaze at higher temperatures hence increasing the mobility of the diffusing elements. Furthermore, it is also possible that free phosphorus may react with CaO from the glaze. In this respect, further work is required in order to evaluate its contribution. Other parameters such as maximum firing temperature and firing time together with the bone china composition are also likely to be important factors in determining the interfacial microstructures produced.

It should be noted that one practical difficulty with the XRD work was to prepare representative specimens of the relevant interfaces in an “interaction layer concentrate” manner. Problems like the unevenness of the surface and different depths of attack also made the assessment of the spectra a difficult task. However, exact identity of the crystalline reaction products formed at the interfaces can be determined satisfactorily by obtaining their corresponding selected area diffraction (SAD) patterns using TEM.

Finally, it is expected that the interactions layers formed at the interfaces during glost firing would manifest themselves in changes in the properties of the glost body, such as mechanical and thermal strength. Further experiments would also be necessary in order to assess such properties in the light of this investigation.

Acknowledgements

The authors would like to thank the Anadolu University (Turkey) for the provision of a scholarship.

References

1. Wozniak, I., Clifford, J. and Wingfield, S., New Cookson Ceramics' unleaded glazes and colours. *Ind. Ceram.*, 1992, **87**(9), 622–627.
2. Cubbon, R. C. P., Consumer and environmental pressures on the use of lead glazes and colours. *Inter-ceram.*, 1994, **43**(4), 240–242.
3. Alsop, S., Development of unleaded glazes for ceramic tableware. *Br. Ceram. Trans.*, 1994, **93**(2), 77–79.
4. Jackson, P. R., Unleaded glazes and colours for tableware- an update. *Br. Ceram. Trans.*, 1995, **94**(4), 171–173.
5. Kara, A. and Stevens, R., Characterisation of biscuit fired bone china body microstructure, I. XRD and SEM of crystalline phases. *J. Eur. Ceram. Soc.*, 2002, **22**(5), 731–736.
6. Kara, A. and Stevens, R., Characterisation of biscuit fired bone china body microstructure, II. Transmission electron microscopy (TEM) of glassy matrix. *J. Eur. Ceram. Soc.*, 2002, **22**(5), 737–743.
7. Roberts, G. J. and Beech, D. G., Glaze-body relationship in bone china. Research Paper No. 433, *Br. Ceram. Res. Assoc.*, 1959.
8. Ichiko, T., A Consideration about the Glazing to the Bone China. *J. Ceram. Soc. Jpn., Int. Ed.*, 1994, **102**(5), 473–477.
9. Monma, H., Goto, M., Nakajima, H. and Hashimoto, H., Preparation of tetracalcium phosphate. *Gypsum and Lime*, 1986, **202**, 151–155.
10. Monma, H. and Kanazawa, T., Reaction mechanism of hydroxyapatite formation in a thermal process. *Nippon Kagaku Kaishi*, 1972, **2**, 339–343.
11. Taylor, J. R. and Bull, A. C., *Ceramic Glaze Technology*. Pergamon Press, Oxford, 1986 (published on behalf of the Institute of Ceramics).
12. Deer, W. A., Howie, R. A. and Zussman, J., *An Introduction to the Rock-Forming Minerals, 6th imp.* Longman Group, London, 1972.
13. Ruddlesten, S. N., The application of electron probe microanalysis to textural studies of ceramics. Research Paper No. 632, *Br. Ceram. Res. Assoc.*, 1971.